

Analysis of chiral and thermal susceptibilities

D. Blaschke*, A. Höll*, C.D. Roberts[†] and S. Schmidt*

**Fachbereich Physik, Universität Rostock, D-18051 Rostock, Germany*

[†]Physics Division, Bldg. 203, Argonne National Laboratory, Argonne IL 60439-4843, USA

(Pacs Numbers: 11.10.Wx, 12.38.Mh, 24.85.+p, 05.70.Fh)

Abstract

We calculate the chiral and thermal susceptibilities for two confining Dyson-Schwinger equation models of QCD with two light flavours, a quantitative analysis of which yields the critical exponents, β and δ , that characterise the second-order chiral symmetry restoration transition. The method itself is of interest, minimising the influence of numerical noise in the calculation of the order parameter for chiral symmetry breaking near the critical temperature. For the more realistic of the two models we find: $T_c \approx 153$ MeV, and the non-mean-field values: $\beta = 0.46 \pm 0.04$, $\delta = 4.3 \pm 0.3$ and $1/(\beta\delta) = 0.54 \pm 0.05$, which we discuss in comparison with the results of other models.

I. INTRODUCTION

Phase transitions are characterised by the behaviour of an order parameter, $\langle X \rangle$, the expectation value of an operator. In the ordered phase of a system: $\langle X \rangle \neq 0$, whereas in the disordered phase $\langle X \rangle = 0$. A phase transition is first-order if $\langle X \rangle \rightarrow 0$ discontinuously, whereas it is second-order if $\langle X \rangle \rightarrow 0$ continuously. For a second-order transition, the length-scale associated with correlations in the system diverges as $\langle X \rangle \rightarrow 0$ and one can define a range of critical exponents that characterise the behaviour of certain macroscopic properties at the transition point. For example, in a system that is ferromagnetic for temperatures less than some critical value, T_c , the magnetisation, M , in the absence of an external magnetic field, behaves as $M \propto (T_c - T)^\beta$ for $T \sim T_c^-$, where β is the critical exponent. At the critical temperature the behaviour of the magnetisation in the presence of an external field, $h \rightarrow 0^+$, defines another critical exponent, δ : $M \propto h^{1/\delta}$. In a system that can be described by mean field theory these critical exponents are

$$\beta^{\text{MF}} = 0.5, \delta^{\text{MF}} = 3.0. \quad (1)$$

Equilibrium, second-order phase transitions can be analysed using the renormalisation group, which leads to scaling laws that reduce the number of independent critical exponents to just two: β and δ [1]. It is widely conjectured that the values of these exponents are fully determined by the dimension of space and the nature of the order parameter. This is the notion of *universality*; i.e., that the critical exponents are *independent* of a theory's microscopic details and hence all theories can be grouped into a much smaller number of universality classes according to the values of their critical exponents. If this is the case, the behaviour of a complicated theory near criticality is completely determined by the behaviour of a simpler theory in the same universality class. So, when presented with an apparently complicated theory, the problem is reduced to only that of establishing its universality class.

Quantum chromodynamics is an asymptotically free theory; i.e., there is an intrinsic, renormalisation-induced mass-scale, Λ_{QCD} , and for squared momentum transfer $Q^2 \gg \Lambda_{\text{QCD}}$, the interactions between quarks and gluons are weaker than Coulombic: $\alpha_s(Q^2) \rightarrow 0$ as $Q^2 \rightarrow \infty$. The study of QCD at finite temperature and baryon number density proceeds via the introduction of the intensive variables: temperature, T ; and quark chemical potential, μ . These are additional mass-scales, with which the coupling can *run* and hence, for $T \gg \Lambda_{\text{QCD}}$ and/or $\mu \gg \Lambda_{\text{QCD}}$, $\alpha_s(Q^2 = 0, T, \mu) \sim 0$. It follows that, at finite temperature and/or baryon number density, there is a phase of QCD in which quarks and gluons are weakly interacting, *irrespective* of the momentum transfer [2]; i.e., a quark-gluon plasma phase. Such a phase of matter existed approximately one microsecond after the big-bang.

At $T, \mu = 0$ the strong interaction is characterised by confinement and dynamical chiral symmetry breaking (DCSB), effects which are tied to the behaviour of $\alpha_s(Q^2)$ at small- Q^2 ; i.e., its long-range behaviour. In a phase of QCD in which the coupling is uniformly small for all Q^2 , these effects are absent and the nature of the strong interaction spectrum is qualitatively different.

The path followed in the transition to the plasma is also important because it determines some observational consequences of the plasma's existence. For example [3], the time-scale for the expansion of the early universe: $\sim 10^{-5}$ s, is large compared with the

natural time-scale in QCD: $1/\Lambda_{\text{QCD}} \sim 1 \text{ fm}/c \sim 10^{-23} \text{ s}$, hence thermal equilibrium is maintained throughout the QCD transition. Therefore if the transition is second-order the ratio $B := \text{baryon-number}/\text{entropy}$, remains unchanged from that value attained at an earlier stage in the universe's evolution. However, a first-order transition would be accompanied by a large increase in entropy density and therefore a reduction in B after the transition. Hence the order of the QCD transition constrains the mechanism for baryon number generation in models describing the formation of the universe, since with a second-order transition this mechanism is only required to produce the presently observed value of B and need not allow for dilution. In the absence of quarks, QCD has a first-order deconfinement transition, while with three or four massless quarks a first-order chiral symmetry restoration transition is expected [3]. What of the realistic case with two light quark flavours?

Based on the global chiral symmetry of QCD with two light quark flavours, it has been argued [3] that this theory and the $N = 4$ Heisenberg magnet are in the same universality class. As a field theory, the $N = 4$ Heisenberg magnet is characterised by an interaction of the form

$$\sum_{i=1}^4 \left\{ \frac{1}{2} \mu^2 \phi_i^2(x) + \frac{1}{4} \lambda^4 \phi_i^4(x) \right\}, \quad (2)$$

where μ^2 is a function of temperature: $\mu^2 \geq 0$ at or above the critical temperature, T_c^H , but $\mu^2 < 0$ for $T < T_c^H$. If the interaction strength, λ , depends smoothly on T and remains positive then, for $T < T_c^H$, the classical minimum of this potential is at

$$\phi_{\text{cl}}^2 = \frac{-\mu^2}{\lambda} > 0. \quad (3)$$

This model is familiar as the nonlinear σ -model, often used to describe low-energy phenomena in QCD. It has been explored thoroughly and has a second order phase transition with critical exponents [4]

$$\beta^H = 0.38 \pm 0.01, \quad \delta^H = 4.82 \pm 0.05. \quad (4)$$

One can examine the hypothesis that this model and QCD with two light quark flavours are in the same universality class via numerical simulations. Such studies on an $8^3 \times 4$ lattice suggest a second-order chiral phase transition with critical exponents [5]

$$\beta^{\text{lat}} = 0.30 \pm 0.08, \quad \delta^{\text{lat}} = 4.3 \pm 0.5 \quad (5)$$

but do not decide the question.¹ These results were obtained through an analysis of the chiral and thermal susceptibilities; a technique that can be applied in the study of any

¹A review [6] of results from more recent simulations on larger lattices with lighter quarks reports a significant dependence of these critical exponents on the lattice volume but with their product approximately constant. A value of $\delta \approx 1$ is obtained, which is characteristic of a first-order transition. These unexpected results might be artefacts of finite lattice spacing because introducing light dynamical quarks drives the simulations to stronger coupling and hence coarser lattices.

theory. Herein we illustrate the method via an analysis of two Dyson-Schwinger equation (DSE) models of QCD, which also allows us to explore the hypothesis further.

Dyson-Schwinger equations provide a renormalisable, nonperturbative, continuum framework for the exploration of strong interaction effects and have been used extensively at $T = 0$ [7] in the study of confinement and DCSB, and in the calculation of hadron observables [8–10]. They have recently [11,12] found successful application at $T \neq 0$ and it is these two models that we employ as exemplars herein. In Sec. II we describe the models and in Sec. III the analysis of their chiral and thermal susceptibilities, and the evaluation of the associated critical exponents. We summarise and conclude in Sec. IV.

II. TWO MODELS

Using a Euclidean metric, with $\{\gamma_\mu, \gamma_\nu\} = 2\delta_{\mu\nu}$ and $\gamma_\mu^\dagger = \gamma_\mu$, the renormalised dressed-quark propagator at $T \neq 0$ takes the form

$$S(p_{\omega_k}) := -i\vec{\gamma} \cdot \vec{p} \sigma_A(p_{\omega_k}) - i\gamma_4 \omega_k \sigma_C(p_{\omega_k}) + \sigma_B(p_{\omega_k}), \quad (6)$$

where $(p_{\omega_k}) := (\vec{p}, \omega_k)$ with $\omega_k = (2k+1)\pi T$ the fermion Matsubara frequency, and $\sigma_{\mathcal{F}}(p_{\omega_k})$, $\mathcal{F} = A, B, C$, are functions only of $|\vec{p}|^2$ and ω_k^2 . The propagator is obtained as a solution of the quark DSE

$$S^{-1}(p_{\omega_k}) := i\vec{\gamma} \cdot \vec{p} A(p_{\omega_k}) + i\gamma_4 \omega_k C(p_{\omega_k}) + B(p_{\omega_k}) \quad (7)$$

$$= Z_2^A i\vec{\gamma} \cdot \vec{p} + Z_2 (i\gamma_4 \omega_k + m_{\text{bm}}) + \Sigma'(p_{\omega_k}), \quad (8)$$

m_{bm} is the Lagrangian current-quark bare mass and the regularised self energy is

$$\Sigma'(p_{\omega_k}) = i\vec{\gamma} \cdot \vec{p} \Sigma'_A(p_{\omega_k}) + i\gamma_4 \omega_k \Sigma'_C(p_{\omega_k}) + \Sigma'_B(p_{\omega_k}), \quad (9)$$

with

$$\Sigma'_{\mathcal{F}}(p_{\omega_k}) = \int_{l,q}^{\bar{\Lambda}} \frac{4}{3} g^2 D_{\mu\nu}(\vec{p} - \vec{q}, \omega_k - \omega_l) \frac{1}{4} \text{tr} [\mathcal{P}_{\mathcal{F}} \gamma_\mu S(q_{\omega_l}) \Gamma_\nu(q_{\omega_l}; p_{\omega_k})], \quad (10)$$

where: $\mathcal{F} = A, B, C$; $\mathcal{P}_A := -(Z_1^A/|\vec{p}|^2) i\vec{\gamma} \cdot \vec{p}$, $\mathcal{P}_B := Z_1$, $\mathcal{P}_C := -(Z_1/\omega_k) i\gamma_4$; and $\int_{l,q}^{\bar{\Lambda}} := T \sum_{l=-\infty}^{\infty} \int^{\bar{\Lambda}} d^3q / (2\pi)^3$, with $\int^{\bar{\Lambda}}$ a mnemonic to represent a translationally invariant regularisation of the integral and $\bar{\Lambda}$ the regularisation mass-scale. In Eq. (10), $\Gamma_\nu(q_{\omega_l}; p_{\omega_k})$ is the renormalised dressed-quark-gluon vertex and $D_{\mu\nu}(\vec{p}, \Omega_k)$ is the renormalised dressed-gluon propagator. ($\Omega_k = 2k\pi T$ is the boson Matsubara frequency.)

In renormalising the quark DSE we require that

$$S^{-1}(p_{\omega_0}) \Big|_{|\vec{p}|^2 + \omega_0^2 = \zeta^2} = i\vec{\gamma} \cdot \vec{p} + i\gamma_4 \omega_0 + m_R, \quad (11)$$

which entails that the renormalisation constants are

$$Z_2^A(\zeta, \bar{\Lambda}) = 1 - \Sigma'_A(\zeta_{\omega_0}^-; \bar{\Lambda}), \quad (12)$$

$$Z_2(\zeta, \bar{\Lambda}) = 1 - \Sigma'_C(\zeta_{\omega_0}^-; \bar{\Lambda}), \quad (13)$$

$$m_R(\zeta) = Z_2 m_{\text{bm}}(\bar{\Lambda}^2) + \Sigma'_B(\zeta_{\omega_0}^-; \bar{\Lambda}), \quad (14)$$

where $(\zeta_{\omega_0}^-)^2 := \zeta^2 - \omega_0^2$, and the renormalised self energies are

$$\mathcal{F}(p_{\omega_k}; \zeta) = \xi_{\mathcal{F}} + \Sigma'_{\mathcal{F}}(p_{\omega_k}; \bar{\Lambda}) - \Sigma'_{\mathcal{F}}(\zeta_{\omega_0}^-; \bar{\Lambda}), \quad (15)$$

$\mathcal{F} = A, B, C$, $\xi_A = 1 = \xi_C$ and $\xi_B = m_R(\zeta)$.

So far no approximations or truncations have been made but to continue we must know the form of $\Gamma_\nu(q_{\omega_l}; p_{\omega_k})$ and $D_{\mu\nu}(\vec{p}, \Omega_k)$ in Eq. (10). These Schwinger functions satisfy DSEs. However, the study of those equations is rudimentary even at $T = 0$ and there are no studies for $T \neq 0$. To proceed we use the $T = 0$ results as a qualitative guide and employ exploratory *Ansätze* for $\Gamma_\nu(q_{\omega_l}; p_{\omega_k})$ and $D_{\mu\nu}(\vec{p}, \Omega_k)$. This is where model parameters enter.

The structure of the dressed fermion-gauge-boson vertex has been much considered [13]. As a connected, irreducible three-point function it should be free of light-cone singularities in covariant gauges; i.e., it should be regular at $(\vec{p} - \vec{q})^2 + (\omega_k - \omega_l)^2 = 0$. A range of *Ansätze* with this property have been proposed and employed [14] and it has become clear that the judicious use of the rainbow truncation

$$\Gamma_\nu(q_{\omega_l}; p_{\omega_k}) = \gamma_\nu \quad (16)$$

in Landau gauge provides reliable results [15]. This is the *Ansatz* employed in Refs. [11,12] and we use it herein. With this truncation a mutually consistent constraint is $Z_1 = Z_2$ and $Z_1^A = Z_2^A$ [15].

With $\Gamma_\nu(q_{\omega_l}; p_{\omega_k})$ regular, the analytic properties of the kernel in the quark DSE are determined by those of $D_{\mu\nu}(p_{\Omega_k})$, which in Landau gauge has the general form

$$g^2 D_{\mu\nu}(p_{\Omega_k}) = P_{\mu\nu}^L(p_{\Omega_k}) \Delta_F(p_{\Omega_k}) + P_{\mu\nu}^T(p_{\Omega_k}) \Delta_G(p_{\Omega_k}), \quad (17)$$

$$P_{\mu\nu}^T(p_{\Omega_k}) \equiv \begin{cases} 0; & \mu \text{ and/or } \nu = 4, \\ \delta_{ij} - \frac{p_i p_j}{p^2}; & \mu, \nu = i, j = 1, 2, 3, \end{cases} \quad (18)$$

with $P_{\mu\nu}^T(p_{\Omega_k}) + P_{\mu\nu}^L(p_{\Omega_k}) = \delta_{\mu\nu} - p_\mu p_\nu / \sum_{\alpha=1}^4 p_\alpha p_\alpha$; $\mu, \nu = 1, \dots, 4$. A “Debye-mass” for the gluon appears as a T -dependent contribution to Δ_F . Considering $D_{\mu\nu}(k)$ at $T = 0$, a perturbative analysis at two-loop order provides a quantitatively reliable estimate for $k^2 > 1\text{-}2 \text{ GeV}^2$, with higher order terms providing corrections of only $\sim 10\%$. However, for $k^2 < 1 \text{ GeV}^2$ nonperturbative methods are necessary. Studies of the gluon DSE in axial gauge [16], where ghost contributions are absent, or in Landau gauge [17], when their contributions are small, indicate that $D_{\mu\nu}(k)$ is significantly enhanced in the vicinity of $k^2 = 0$ relative to a free gauge-boson propagator, and that the enhancement persists to $k^2 \sim 1 \text{ GeV}^2$. Due to the truncations involved these studies are not quantitatively reliable but this behaviour has been modelled successfully as a distribution located in the vicinity of $k^2 = 0$ [15,18].

A. Infrared-dominant Model

A particularly simple and illustratively useful model is obtained with

$$\Delta_F(p_{\Omega_k}) = \Delta_G(p_{\Omega_k}) = 2\pi^3 \frac{\eta^2}{T} \delta_{k0} \delta^3(\vec{p}), \quad (19)$$

which is a generalisation to $T \neq 0$ of the model introduced in Ref. [19], where $\eta \approx 1.06$ GeV is a mass-scale parameter fixed by fitting π - and ρ -meson masses. As an infrared-dominant model Eq. (19) does not represent well the behaviour $D_{\mu\nu}(p_{\Omega_k})$ away from $p_{\Omega_k}^2 \simeq 0$, and hence there are some model-dependent artefacts. However, these artefacts are easily identified and, because of its simplicity, the model has provided a useful means of elucidating many of the qualitative features of more sophisticated *Ansätze*.

Using Eqs. (16) and (19) the quark DSE is ultraviolet-finite, the cutoff can be removed and the renormalisation point taken to infinity, so that Eq. (8) becomes the algebraic equations

$$\eta^2 m^2 = B^4 + m B^3 + (4p_{\omega_k}^2 - \eta^2 - m^2) B^2 - m (2\eta^2 + m^2 + 4p_{\omega_k}^2) B, \quad (20)$$

$$A(p_{\omega_k}) = C(p_{\omega_k}) = \frac{2B(p_{\omega_k})}{m + B(p_{\omega_k})}, \quad (21)$$

with $Z_2^A = 1 = Z_2$ and $m = m_R = m_{\text{bm}}$: $m = 0$ defines the chiral limit. This DSE-model of QCD has coincident, second-order deconfinement and chiral symmetry restoration phase transitions at a critical temperature $T_c^{\text{IR}} \approx 0.16 \eta$ [12].

B. Ultraviolet-improved Model

An improvement over Eq. (19) is obtained by correcting the large- $p_{\Omega_k}^2$ behaviour so as to better represent the interaction at short-distances. The one-parameter model

$$\Delta_F(p_{\Omega_k}) = \mathcal{D}(p_{\Omega_k}; m_D), \quad (22)$$

$$\Delta_G(p_{\Omega_k}) = \mathcal{D}(p_{\Omega_k}; 0), \quad (23)$$

$$\mathcal{D}(p_{\Omega_k}; m) := \frac{16}{9} \pi^2 \left[\frac{2\pi}{T} m_t^2 \delta_{0k} \delta^3(\vec{p}) + \frac{1 - e^{[-(|\vec{p}|^2 + \Omega_k^2 + m^2)/(4m_t^2)]}}{|\vec{p}|^2 + \Omega_k^2 + m^2} \right], \quad (24)$$

where $m_D^2 = (8/3) \pi^2 T^2$ is the perturbatively evaluated “Debye-mass”², achieves this. This gluon propagator provides a generalisation to $T \neq 0$ of the model explored in Ref. [18] where the parameter m_t is a mass-scale that marks the boundary between the perturbative and nonperturbative domains. The value $m_t = 0.69$ GeV = 1/0.29 fm is fixed by requiring a good description of a range of π - and ρ -meson properties. In this case the DSE yields a pair of coupled, nonlinear integral equations that must be solved subject to the renormalisation boundary conditions, and $m_R = 0$ defines the chiral limit. This model also has coincident, second-order deconfinement and chiral symmetry restoration transitions, with the critical temperature $T_c^{\text{UV}} \approx 0.15$ GeV [11].

²The influence of the Debye-mass on finite- T observables is qualitatively unimportant, even in the vicinity of the chiral symmetry restoration transition. The ratio of the coefficients in the two terms in Eq. (24) is such that the long-range effects associated with $\delta_{0k} \delta^3(p)$ are completely cancelled at short-distances; i.e., for $|\vec{x}|^2 m_t^2 \ll 1$.

III. CHIRAL AND THERMAL SUSCEPTIBILITIES

In the study of dynamical chiral symmetry breaking an order parameter often used is the quark condensate, $\langle \bar{q}q \rangle_\zeta$. In QCD in the chiral limit this order parameter is defined via the quark propagator [15]:

$$-\langle \bar{q}q \rangle_\zeta := N_c \lim_{\bar{\Lambda} \rightarrow \infty} Z_4(\zeta, \bar{\Lambda}) \int_{l,q}^{\bar{\Lambda}} \frac{B_0(p_{\omega_l})}{|\vec{p}|^2 A_0(p_{\omega_l})^2 + \omega_l^2 C_0(p_{\omega_l})^2 + B_0(p_{\omega_l})^2}, \quad (25)$$

for each massless quark flavour, where the subscript “0” denotes that the scalar functions: A_0 , B_0 , C_0 , are obtained as solutions of Eq. (8) in the chiral limit, and $Z_4(\zeta, \bar{\Lambda})$ is the mass renormalisation constant: $Z_4(\zeta, \bar{\Lambda}) m_R(\zeta) = Z_2(\zeta, \bar{\Lambda}) m_{\text{bm}}(\bar{\Lambda})$. The functions have an implicit ζ -dependence. From Eq. (25) it is clear that an equivalent order parameter for the chiral transition is

$$\mathcal{X} := B_0(\vec{p} = 0, \omega_0), \quad (26)$$

which was used in Refs. [11,12]. Thus the zeroth Matsubara mode determines the character of the chiral phase transition, a conjecture explored in Ref. [20].

To accurately characterise the chiral symmetry restoration transitions in the two models introduced above, we examine closely the chiral and thermal susceptibilities and their scaling behaviour near the critical point. This allows a determination of the critical temperature, T_c , and exponents β and δ , as we explain in the appendix. In the notation of the appendix, the “magnetisation” is

$$M(t, h) := B(\vec{p} = 0, \omega_0), \quad (27)$$

i.e., the value in the infrared of the scalar piece of the quark self energy obtained as the m_R - and T -dependent solution of Eq. (8).

A. Critical Exponents of the Infrared-dominant Model

In the chiral limit, Eq. (20) has the Nambu-Goldstone mode solution

$$B(p_{\omega_k}) = \begin{cases} \sqrt{\eta^2 - 4p_{\omega_k}^2}, & p_{\omega_k}^2 < \frac{\eta^2}{4} \\ 0, & \text{otherwise} \end{cases} \quad (28)$$

$$C(p_{\omega_k}) = \begin{cases} 2, & p_{\omega_k}^2 < \frac{\eta^2}{4} \\ \frac{1}{2} \left(1 + \sqrt{1 + \frac{2\eta^2}{p_{\omega_k}^2}} \right), & \text{otherwise,} \end{cases} \quad (29)$$

and hence

$$M(t, 0) = 2\pi \left(\frac{\eta}{2\pi} + T \right)^{\frac{1}{2}} \left(\frac{\eta}{2\pi} - T \right)^{\frac{1}{2}}. \quad (30)$$

From Eq. (30) we read that

$$T_c^{\text{IR}} = \frac{\eta}{2\pi} \approx 0.159155 \eta, \quad \beta^{\text{IR}} = \frac{1}{2}. \quad (31)$$

To determine δ we use Eq. (20) at $T = T_c$ to obtain

$$\eta^2 m^2 = M(0, h)^4 + m M(0, h)^3 + m^2 M(0, h)^2 - m(3\eta^2 + m^2) M(0, h) \quad (32)$$

and suppose that, for $m \sim 0$, $M(0, h) = a m^{1/\delta}$. Consistency requires

$$\delta^{\text{IR}} = 3. \quad (33)$$

That the chiral symmetry restoration transition in this model is characterised by mean field critical exponents is not surprising because the interaction described by Eq. (19) is a constant in configuration space. Mean field critical exponents are also obtained in chiral random matrix models of QCD [20,21].

To illustrate the evaluation of the critical temperature and exponents using the chiral and thermal susceptibilities we use Eqs. (20), (A9) and (A10) to obtain

$$\chi_h(T, h) = -\frac{2 M(T, h) T b_- [1 - M(T, h) b_-] - M(T, h) T b_+}{2 M(T, h) b_- b_+ [1 - M(T, h) b_-] - b_- b_+ - M(T, h) b_-}, \quad (34)$$

$$\chi_T(T, h) = \frac{8\pi^2 T M(T, h)^2 b_-^2 - 2 M(T, h) b_- b_+ h [1 - M(T, h) b_-] - M(T, h) h b_+^2}{2 M(T, h) b_- b_+ [1 - M(T, h) b_-] - b_- b_+ - M(T, h) b_-}, \quad (35)$$

where $b_{\pm} := M(T, h) \pm hT$. In Fig. 1 we plot the chiral susceptibility. The temperature dependence is typical of this quantity, with the peak increasing in height and becoming narrower as $h \rightarrow 0^+$; i.e., as the external source for chiral symmetry breaking is removed. To understand this behaviour, recall that the chiral susceptibility is the derivative of the order parameter with-respect-to the explicit chiral symmetry breaking mass. Denote the typical mass-scale associated with DCSB by M_{χ} . For $h \gg M_{\chi}$, explicit chiral symmetry breaking dominates, with the order parameter $\mathcal{X} \sim h$ and insensitive to T , and hence $\chi_h \approx \text{const.}$ For $h \sim M_{\chi}$, \mathcal{X} begins to vary with T because the origin of its magnitude changes from the explicit mass to the DCSB mechanism as T passes through the pseudocritical temperature, T_{pc}^h . This is reflected in χ_h as the appearance of a peak at T_{pc}^h . For $h \ll M_{\chi}$, $\mathcal{X} \sim h$ until very near T_{pc}^h when the scale of DCSB overwhelms h and $\mathcal{X} \sim M_{\chi}$. The change in \mathcal{X} is rapid leading to the behaviour observed in χ_h . The thermal susceptibility is plotted in Fig. 2 and has qualitatively similar features.

In Table I we present the pseudocritical points and peak heights obtained for h in the scaling window, defined as the domain of h for which

$$\frac{t_{\text{pc}}^h}{t_{\text{pc}}^t} = \text{const.}; \quad (36)$$

i.e., the values of h for which Eqs. (A15) and (A16) are valid. Based on Eqs. (A17) and (A18), using the tabulated values, one obtains z_h^{IR} and z_t^{IR} from linear fits to the curves: $\log \chi_h^{\text{pc}}$ -versus- $\log h$ and $\log \chi_T^{\text{pc}}$ -versus- $\log h$, respectively. This yields

$$z_h^{\text{IR}} = 0.666, \quad z_t^{\text{IR}} = 0.335, \quad (37)$$

and hence $\beta_\chi^{\text{IR}} = 0.499$ and $\delta_\chi^{\text{IR}} = 2.99$, as listed in Table II. These values are in excellent agreement with the exact (mean field) results, Eqs. (31) and (33). With the value of

$$\frac{1}{(\beta\delta)^{\text{IR}}} = 1 - z_h^{\text{IR}} + z_t^{\text{IR}} = 0.670, \quad (38)$$

T_c^{IR} can be obtained in a variational procedure based on Eq. (A15): it is that value which minimises the standard deviation between $\log(T_{\text{pc}}^h - T_c^{\text{IR}}) - 1/(\beta\delta)^{\text{IR}} \log h$ and a constant. This yields $T_c^{\text{IR}} = 0.159155\eta$ again in excellent agreement with Eq. (31). The value in Table II is obtained with $\eta = 1.06 \text{ GeV}$ [19]. Applying the same procedure to $\log(T_{\text{pc}}^T - T_c^{\text{IR}}) - 1/(\beta\delta)^{\text{IR}} \log h$, yields $T_c^{\text{IR}} = 0.159151\eta$.

B. Critical Exponents of the Ultraviolet-improved Model

In this case the quark DSE must be solved numerically, as in Refs. [11,18]. In these calculations we used a 3-momentum grid with 96 points and we renormalised at $\zeta = 9.47 \text{ GeV}$, the value at which the parameter $m_t (= 0.69 \text{ GeV})$ was fixed [18]. The chiral and thermal susceptibilities for a range of values of h are plotted in Figs. 3 and 4, and the pseudocritical points and peak heights obtained for values of h in the scaling window are presented in Table III.

As observed in Sec. III A, one obtains z_h^{UV} and z_t^{UV} from linear fits to the curves $\log \chi_h^{\text{pc}}$ -versus- $\log h$ and $\log \chi_T^{\text{pc}}$ -versus- $\log h$, respectively. The data and fits are presented in Fig. 5 and yield

$$z_h^{\text{UV}} = 0.77 \pm 0.02, \quad z_t^{\text{UV}} = 0.28 \pm 0.04, \quad (39)$$

with the corresponding results for β and δ listed in the first column of Table II.³ For this model only, as a check and demonstration of consistency, the values of T_c^{UV} and $1/(\beta\delta)^{\text{UV}}$ were calculated using a variational procedure based on Eqs. (A15) and (A16): the values of T_c^{UV} and $1/(\beta\delta)^{\text{UV}}$ were varied in order to minimise the standard deviation in a linear fit to $\log(T_{\text{pc}} - T_c^{\text{UV}}) - 1/(\beta\delta)^{\text{UV}} \log h$. The difference between using T_{pc}^h and T_{pc}^T is less than the error quoted in the table.

In Ref. [11] the values of β and T_c in the ultraviolet-improved model were calculated directly from the magnetisation order parameter; i.e., using Eq. (A6), with the results $\beta = 0.33 \pm 0.3$ and $T_c \approx 152 \text{ MeV}$. There is a discrepancy in the value of β . We expect that the result obtained herein is more accurate because our method avoids the numerical noise associated with establishing the precise behaviour of the order parameter in the vicinity of the critical temperature.

³Our quoted error bounds the slope of the linear fit. It is calculated from the slope of linear fits to the two endpoint values when they are displaced vertically, in opposite directions, by the standard deviation of the fit to all the tabulated results.

IV. SUMMARY AND CONCLUSIONS

A primary purpose of this study was an illustration of the method by which one can calculate the critical exponents that characterise a chiral symmetry restoration transition, β and δ , using the chiral and thermal susceptibilities. For this purpose we chose two Dyson-Schwinger equation models of two-light-flavour QCD that have been applied successfully [11,12,22] in phenomenological studies of QCD at finite temperature and density. The method is reliable and should have a wide range of application because it is more accurate in the presence of numerical noise than a straightforward analysis of the chiral symmetry (magnetisation) order parameter.

We established that our finite temperature extension of the infrared-dominant model of Ref. [19] is characterised by mean field critical exponents, listed in Table II. It is therefore not in the universality class expected [3,5] of two-light-flavour lattice-QCD. However, the critical temperature is consistent with that estimated in lattice simulations. This fits an emerging pattern that DSE models whose mass-scale parameters are fixed by requiring a good description of hadron observables at $T = 0$, yield a reliable estimate of the critical temperature for chiral symmetry restoration. It is a quantity that is not too sensitive to details of the model.

Consistent with this observation, the critical temperature in the ultraviolet improved model of Ref. [18] also agrees with that estimated in lattice simulations. The critical exponent δ agrees with the value obtained for two-light-flavour lattice-QCD and is consistent with that of the $N = 4$ Heisenberg magnet. However, the difference between the value of β obtained in the model and that in lattice simulations is significant. It is unlikely that numerical errors in our study are the cause of this discrepancy. The values of the critical exponents, and their product, establish that this model is not mean field in character. They also establish that the ultraviolet-improved model, which provides a good description of low-energy π - and ρ -observables, is not in the same universality class as the $N = 4$ Heisenberg magnet.

The difference between the infrared-dominant model and the ultraviolet-improved one is the value of m_t ; i.e., the mass scale that marks the boundary between strong and weak coupling. In the limit $m_t \rightarrow \infty$, the infrared-dominant model is recovered from the ultraviolet-improved one: in this limit the interaction is always strong. Our results therefore demonstrate that the critical exponents are sensitive to the particular manner in which the theory makes the transition from strong to weak coupling. This should be expected since that evolution is a determining characteristic of the β -function of a renormalisable theory, one which a chiral symmetry restoration transition must be sensitive to.

The large- p^2 behaviour of the gluon propagator in the ultraviolet-improved model, although better than that in the infrared-dominant model, is still inadequate. Its renormalisation group properties are more like those of quenched-QED than QCD because of the absence of the logarithmic suppression of the running coupling characteristic of asymptotically free theories. This is corrected in the model of Ref. [15], which has more in common with QCD at $T = 0$ and whose finite temperature properties can therefore assist in better understanding the details of the chiral symmetry restoration transition in two-light-flavour QCD.

ACKNOWLEDGMENTS

D.B. and S.S. acknowledge the hospitality of the Physics Division at Argonne National Laboratory, and C.D.R. that of the Department of Physics at the University of Rostock during visits in which parts of this work were conducted. We are also grateful to the faculty and staff at JINR-Dubna for their hospitality during the workshop on *Deconfinement at Finite Temperature and Density* in October 1997. This work was supported in part by Deutscher Akademischer Austauschdienst; the US Department of Energy, Nuclear Physics Division, under contract number W-31-109-ENG-38; the National Science Foundation under grant no. INT-9603385; and benefited from the resources of the National Energy Research Scientific Computing Center.

APPENDIX: CRITICAL EXPONENTS FROM SUSCEPTIBILITIES

Consider the free energy of a theory, represented by

$$f = f(t, h), \quad (\text{A1})$$

where $t := T/T_c - 1$ is the reduced temperature and $h := m/T$ is the explicit source of chiral symmetry breaking measured in units of the temperature; it is analogous to an external magnetic field. Since correlation lengths diverge in a second-order transition it follows that for $t, h \rightarrow 0$ the free energy is a generalised homogeneous function; i.e.,

$$f(t, h) = \frac{1}{b} f(t b^{y_t}, h b^{y_h}). \quad (\text{A2})$$

This entails the following behaviour of the “magnetisation”

$$M(t, h) := \left. \frac{\partial f(t, h)}{\partial h} \right|_{t \text{ fixed}}, \quad (\text{A3})$$

$$M(t, h) = b^{y_h - 1} M(t b^{y_t}, h b^{y_h}). \quad (\text{A4})$$

The scaling parameter, b , is arbitrary and along the trajectory $|t|b^{y_t} = 1$ one has

$$M(t, h) = |t|^{(1-y_h)/y_t} M(\text{sgn}(t), h |t|^{-y_h/y_t}), \quad (\text{A5})$$

$$M(t, 0) \propto |t|^\beta, \quad \beta := \frac{1 - y_h}{y_t}. \quad (\text{A6})$$

Alternatively, along the trajectory $h b^{y_h} = 1$

$$M(t, h) = h^{(1-y_h)/y_h} M(t h^{-y_t/y_h}, 1), \quad (\text{A7})$$

$$M(0, h) \propto h^{1/\delta}, \quad \delta := \frac{y_h}{1 - y_h}. \quad (\text{A8})$$

This defines the critical behaviour and provides that direct means of extracting the critical exponent β employed in Refs. [11,12]. However, because of numerical noise, it can be difficult to extract quantitatively accurate results using this method.

The critical exponents can also be determined by studying the pseudocritical behaviour of the chiral and thermal susceptibilities, defined respectively as

$$\chi_h(t, h) := \left. \frac{\partial M(t, h)}{\partial h} \right|_{t \text{ fixed}}, \quad (\text{A9})$$

$$\chi_t(t, h) := \left. \frac{\partial M(t, h)}{\partial t} \right|_{h \text{ fixed}}. \quad (\text{A10})$$

For convenience, we often use $\chi_T(T, h) := (1/T_c) \chi_t(t, h)$.

For $t, h \rightarrow 0^+$, along $hb^{y_h} = 1$, one has

$$\chi_h(t, h) = h^{(1-2y_h)/y_h} \chi_h(t h^{-y_t/y_h}, 1), \quad (\text{A11})$$

$$\chi_t(t, h) = h^{(1-y_h-y_t)/y_h} \chi_t(t h^{-y_t/y_h}, 1). \quad (\text{A12})$$

At each h , $\chi_h(t, h)$ and $\chi_t(t, h)$ are smooth functions of t . Suppose they have maxima at t_{pc}^h and t_{pc}^t , respectively, described as the pseudocritical points. Consider the chiral susceptibility. At its maximum

$$0 = \left. \frac{\partial}{\partial t} \chi_h(t, h) \right|_{t_{\text{pc}}^h} \quad (\text{A13})$$

$$= h^{(1-2y_h)/y_h} \left. \frac{\partial}{\partial t} (t h^{-y_t/y_h}) \left[\frac{\partial}{\partial z} \chi_h(z, 1) \right] \right|_{z=t h^{-y_t/y_h}} \bigg|_{t_{\text{pc}}^h}, \quad (\text{A14})$$

which entails that

$$t_{\text{pc}}^h = K_h h^{y_t/y_h} = K_h h^{1/(\beta\delta)}, \quad (\text{A15})$$

where K_h is an undetermined constant. Similarly,

$$t_{\text{pc}}^t = K_t h^{y_t/y_h} = K_t h^{1/(\beta\delta)}. \quad (\text{A16})$$

Since $\beta\delta > 0$, it follows that the pseudocritical points approach the critical point, $t = 0$, as $h \rightarrow 0^+$. It follows from Eqs. (A15) and (A16) that at the pseudocritical points

$$\chi_h^{\text{pc}} := \chi_h(t_{\text{pc}}^h, h) \propto h^{-z_h}, \quad z_h := 1 - \frac{1}{\delta}, \quad (\text{A17})$$

$$\chi_t^{\text{pc}} := \chi_t(t_{\text{pc}}^t, h) \propto h^{-z_t}, \quad z_t := \frac{1}{\beta\delta} (1 - \beta). \quad (\text{A18})$$

Thus by locating the pseudocritical points and plotting the peak-height of the susceptibilities as a function of h one can obtain values of T_c , β and δ .

REFERENCES

- [1] R. J. Creswick, H. A. Farach and C. P. Poole, *Introduction to Renormalization Group Methods in Physics* (John Wiley and Sons, Inc., New York, 1992).
- [2] J. C. Collins and M. J. Perry, Phys. Rev. Lett. **34**, 1353 (1975)
- [3] K. Rajagopal, “The Chiral Phase Transition in QCD: Critical Phenomena and Long-wavelength Pion Oscillations”, in *Quark-gluon plasma*, ed. R. C. Hwa (World Scientific, New York, 1995), 484.
- [4] G. Baker, B. Nickel and D. Meiron, Phys. Rev. B **17**, 1365 (1978); and “Compilation of 2-pt. and 4-pt. graphs for continuous spin models”, University of Guelph report (1977), unpublished.
- [5] F. Karsch and E. Laermann, Phys. Rev. D **50**, 6954 (1994).
- [6] E. Laermann, “Thermodynamics using Wilson and Staggered Quarks”, hep-lat/9802030.
- [7] C.D. Roberts and A.G. Williams, Prog. Part. Nucl. Phys. **33**, 477 (1994).
- [8] P. C. Tandy, Prog. Part. Nucl. Phys. **39**, 117 (1997).
- [9] M. A. Pichowsky and T.-S. H. Lee, Phys. Rev. D **56**, 1644 (1997).
- [10] M. A. Ivanov, Yu. L. Kalinovsky, P. Maris and C. D. Roberts, “Heavy- to light-meson transition form factors”, nucl-th/9711023, Phys. Rev. C, April (1998).
- [11] A. Bender, D. Blaschke, Yu. Kalinovsky and C.D. Roberts, Phys. Rev. Lett. **77**, 3724 (1996).
- [12] D. Blaschke, C.D. Roberts and S. Schmidt, “Thermodynamic properties of a simple, confining model”, nucl-th/9706070, Phys. Lett. B, in press.
- [13] A. Bashir, A. Kizilersu and M.R. Pennington, Phys. Rev. D **57**, 1242 (1998).
- [14] F. T. Hawes, C. D. Roberts and A. G. Williams, Phys. Rev. D **49**, 4683 (1994).
- [15] P. Maris and C. D. Roberts, Phys. Rev. C **56**, 3369 (1997).
- [16] M. Baker, J. S. Ball and F. Zachariasen, Nucl. Phys. B **186** 531 (1981); *ibid* 560; D. Atkinson, P. W. Johnson, W. J. Schoenmaker and H. A. Slim, Nuovo Cimento A **77**, Series 11 (1983) 197.
- [17] N. Brown and M. R. Pennington, Phys. Rev. D **39**, 2723 (1989); M. R. Pennington, “Calculating hadronic properties in strong QCD”, hep-ph/9611242.
- [18] M.R. Frank and C.D. Roberts, Phys. Rev. C **53**, 390 (1996).
- [19] H.J. Munczek and A.M. Nemirovsky, Phys. Rev. D **28**, 3081 (1983).
- [20] A. D. Jackson and J. J. M. Verbaarschot, Phys. Rev. D **53**, 7223 (1996).
- [21] T. Wettig, T. Guhr, A. Schäfer and H. A. Weidenmüller, in *QCD Phase Transitions*, Proceedings of the XXVth International Workshop on Gross Properties of Nuclei and Nuclear Excitations, Hirschegg, Austria (1997), edited by H. Feldmeier, J. Knoll, W. Nörenberg and J. Wambach, hep-ph/9701387.
- [22] A. Bender, G. Poulis, C.D. Roberts, S. Schmidt and A.W. Thomas, “Deconfinement at finite chemical potential”, nucl-th/971009.

TABLES

$\log h$	T_{pc}^h/η	χ_h^{pc}/η	T_{pc}^T/η	χ_T^{pc}
-5.0	0.15921	707.0	0.15917	248.5
-4.3	0.15931	241.9	0.15920	145.4
-4.0	0.15941	152.9	0.15923	115.3
-3.3	0.15990	52.19	0.15939	67.33
-3.0	0.16034	32.91	0.15953	53.34
-2.3	0.16268	11.31	0.16052	30.91

TABLE I. The pseudocritical points and peak heights for the chiral and thermal susceptibilities in the infrared-dominant model, obtained from Eqs. (34) and (35) respectively.

	IR Dominant	UV Improved	O(4)	Lattice
δ	3.0	4.3 ± 0.3	4.82 ± 0.05	4.3 ± 0.5
β	0.50	0.46 ± 0.04	0.38 ± 0.01	0.30 ± 0.08
$\frac{1}{\beta\delta}$	0.67	0.54 ± 0.05	0.55 ± 0.02	0.77 ± 0.14
T_c (MeV)	168.7	153.5 ± 0.1	—	140 ... 160

TABLE II. Critical exponents and temperature for the models considered herein and a comparison with the results in the $N = 4$ Heisenberg magnet [4], labelled as O(4), and lattice simulations of QCD with two light flavours [5].

$\log h$	T_{pc}^h (GeV)	χ_h^{pc} (GeV)	T_{pc}^T (GeV)	χ_T^{pc}
-4.30	0.15464	896.3	0.15379	67.72
-4.00	0.15515	530.7	0.15394	55.70
-3.70	0.15571	303.8	0.15422	45.70
-3.52	0.15627	224.9	0.15443	40.65
-3.40	0.15677	181.8	0.15460	37.37
-3.30	0.15729	154.9	0.15487	35.00
-3.15	0.15795	120.3	0.15508	31.64
-3.04	0.15840	97.21	0.15534	29.32
-3.0	0.15872	90.03	0.15536	28.39

TABLE III. The pseudocritical points and peak heights for the chiral and thermal susceptibilities in the ultraviolet-improved model, obtained from the numerical solution of Eq. (8) with the gluon propagator of Eqs. (22)–(24). From the dependence of the peak heights on the number of points in the \vec{p} -array, we estimate a systematic 1.5% error in χ_h^{pc} and 10% in χ_T^{pc} .

FIGURES

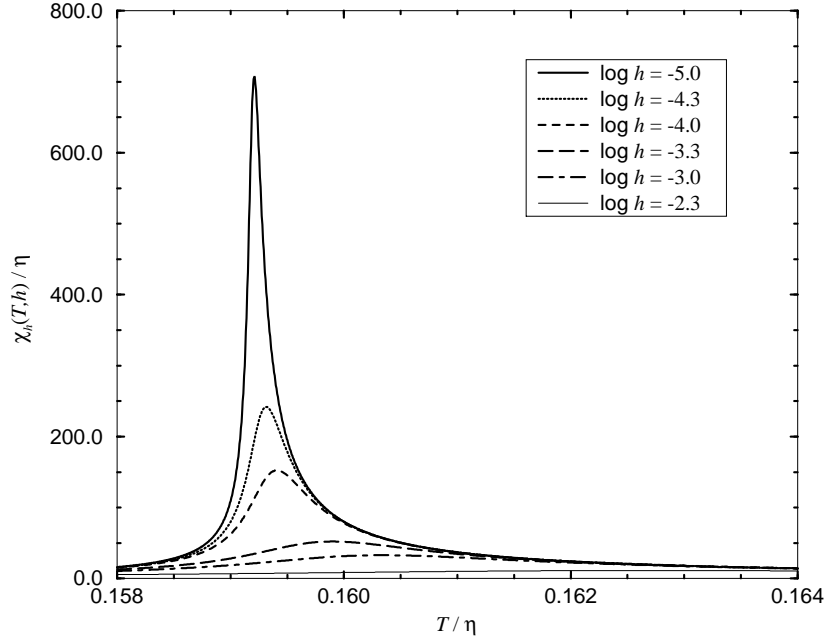


FIG. 1. The chiral susceptibility, $\chi_h(T, h)$, in the infrared-dominant model, Eq. (34), as a function of T for various values of h .

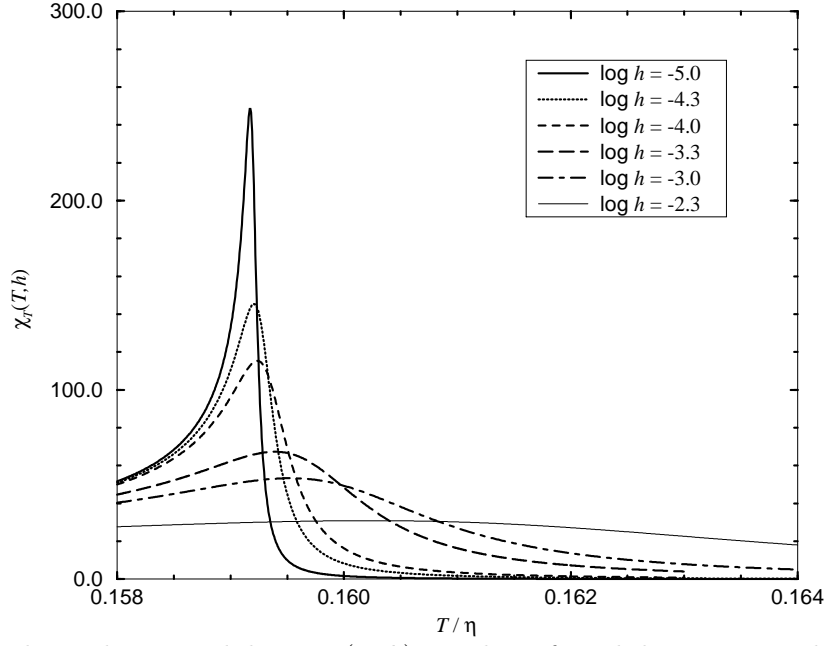


FIG. 2. The thermal susceptibility, $\chi_T(T, h)$, in the infrared-dominant model, Eq. (35), as a function of T for various values of h .

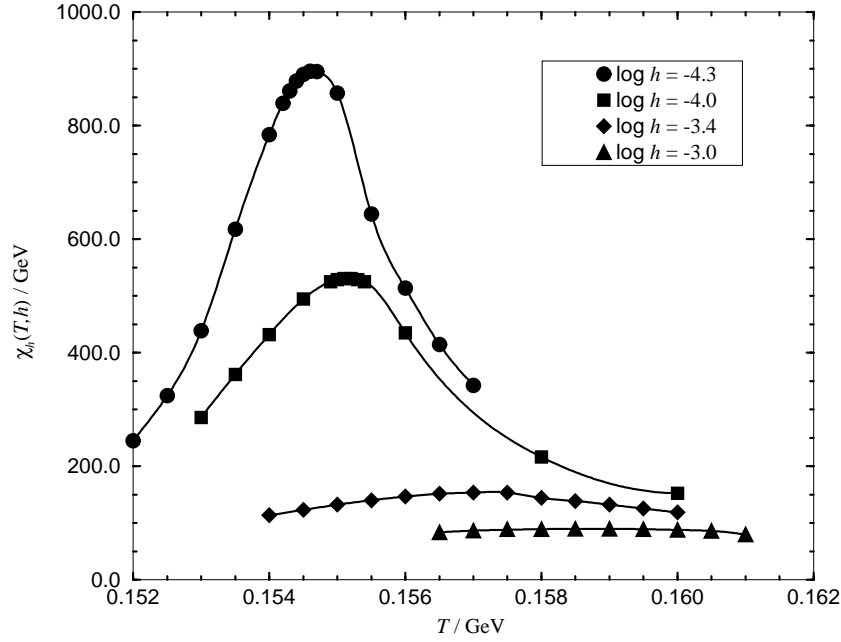


FIG. 3. The chiral susceptibility, $\chi_h(T, h)$, in the ultraviolet-improved model, Sec. IIB, as a function of T for various values of h .

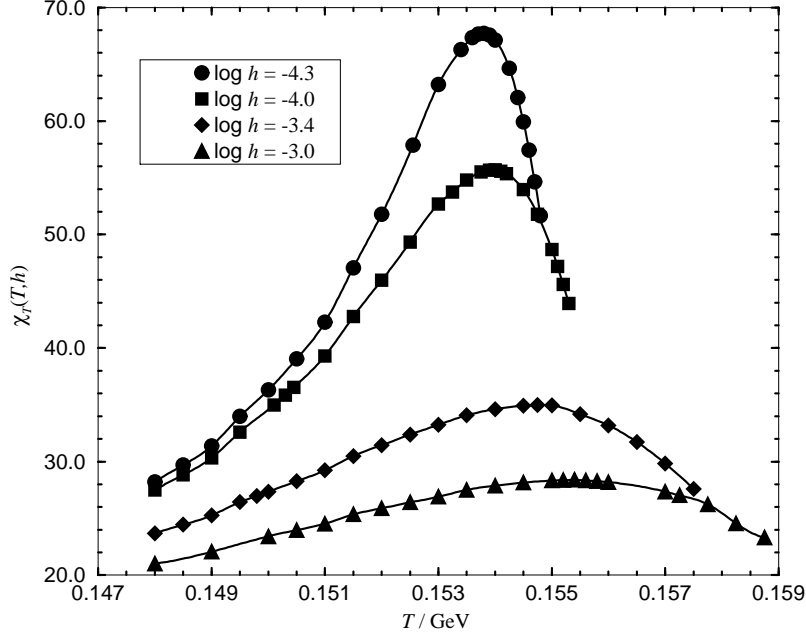


FIG. 4. The thermal susceptibility, $\chi_T(T, h)$, in the ultraviolet-improved model, Sec. IIB, as a function of T for various values of h .

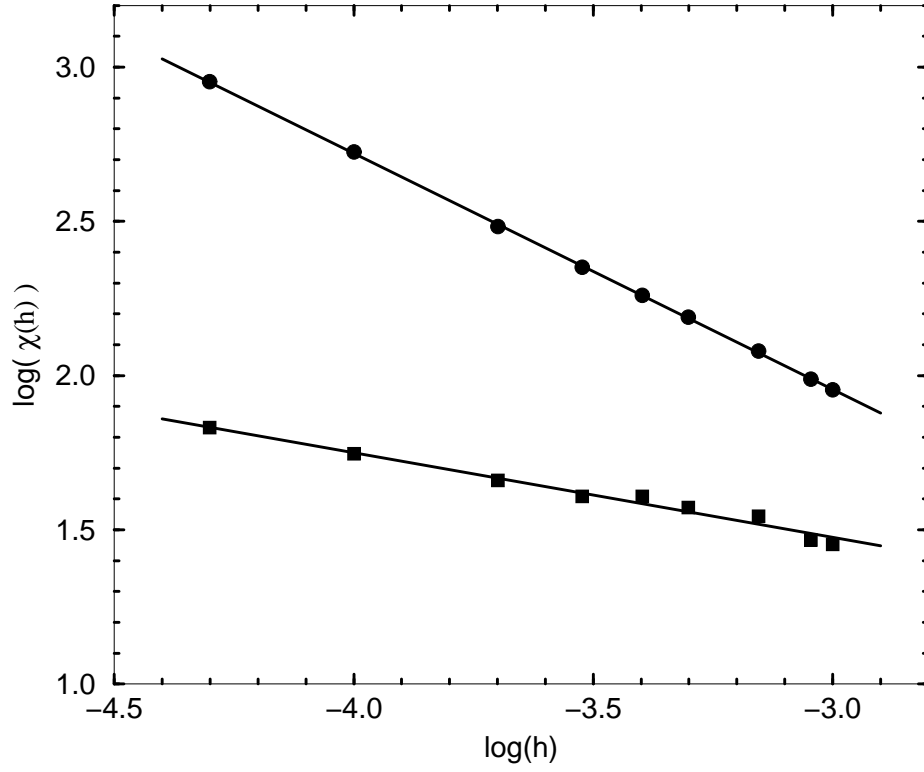


FIG. 5. The peak heights at the pseudocritical points of the chiral and thermal susceptibilities in the ultraviolet-improved model: χ_h^{pc} (filled-circles), χ_T^{pc} (filled squares). The solid lines are straight-line fits, with the slopes $-z_h^{\text{UV}}$ and $-z_t^{\text{UV}}$ given in Eq. (39), which verify the scaling laws in Eqs. (A17) and (A18).